Multifragmentation of heavy systems: characteristics and scaling laws

M.F. Rivet, Ch.O. Bacri, B. Borderie, J.D. Frankland, M. Squalli, R. Bougault, S. Salou, A. Chbihi, J.P. Wieleczko, M. Assenard, et al.

18 mars 1997

IPNO-DRE-97-11
GANIL P 97 08
LYCEN/9710

CEA/DAPNIA/SPhN 97-16
LPCC 97-05
SUBATECH-97-07

MULTIFRAGMENTATION OF HEAVY SYSTEMS :
Characteristics and scaling laws

M.F. RIVET for the INDRA collaboration

Invited talk to the XXXV Int. Winter Meeting on Nuclear Physics, Bormio (Italy), February 3-7, 1997

MULTIFRAGMENTATION OF HEAVY SYSTEMS: Characteristics and scaling laws

Marie-France Rivet

for the INDRA collaboration

Ch.O. Bacri[1], B. Borderie[1], J.D. Frankland[1], M. Squalli[1], R. Bougault[3], S. Salou[2], A. Chbihi[2], J.P. Wieleczko[2], M. Assenard[6], G. Auger[2], J. Benlliure[2], E. Bisquer[4], F. Bocage[3], R. Brou[3], P. Buchet[5], J.L. Charvet[5], J. Colin[3], D. Cussol[3], R. Dayras[5], E. De Filippo[5], A. Demeyer[4], D. Doré[1], D. Durand[3], P. Eudes[6], E. Galichet[4], E. Genouin-Duhamel[3], E. Gerlic[4], M. Germain[6], D. Gourio[6], D. Guinet[4], P. Lautesse[4], J.L. Laville[6], J.F. Lecolley[3], A. Le Fèvre[2], T. Lefort[3], R. Legrain[5], O. Lopez[3], M. Louvel[3], N. Marie[2], V. Métivier[6], L. Nalpas[5], A.D. Nguyen[3], M. Parlog[7], J. Péter[3], E. Plagnol[1], A. Rahmani[6], T. Reposeur[6], E. Rosato[8], R. Roy[9], F. Saint-Laurent[2], J.C. Steckmeyer[3], M. Stern[4], G. Tabacaru[7], B. Tamain[3], O. Tirel[2], L. Tassan-Got[1], E. Vient[3], C. Volant[5].

and

Ph. Chomaz[2], M. Colonna[2], A. Guarnera[2]

[1] *Institut de Physique Nucléaire, IN2P3-CNRS, 91406 Orsay Cedex, France.*

[2] *GANIL, CEA, IN2P3-CNRS, B.P. 5027, 14021 Caen Cedex, France.*

[3] *LPC, IN2P3-CNRS, ISMRA et Université, 14050 Caen Cedex, France.*

[4] *IPN Lyon, IN2P3-CNRS et Université, 69622 Villeurbanne Cedex, France.*

[5] *CEA, DAPNIA/SPhN, CEN Saclay, 91191 Gif sur Yvette Cedex, France.*

[6] *SUBATECH, IN2P3-CNRS et Université, 44072 Nantes Cedex 03, France.*

[7] *Institute of Physics and Nuclear Engineering, IFA, P.O. Box MG6, Bucharest, Romania.*

[8] *Dipartimento di Scienze, Univ. di Napoli, 80125 Napoli, Italy.*

[9] *Laboratoire de Physique Nucléaire, Département de Physique, Université Laval, Québec G1K7P4, Canada.*

Abstract

Multifragmentation of heavy systems has been studied for different target-projectile couples between 30 and 50 AMeV. The formation of a transient system containing essentially all the nucleons of the incident nuclei, which subsequently undergoes multifragmentation while expanding, is demonstrated. The characteristics of the process are studied, among which the evolution of the expansion energy, the size of the fragments, the shape of the fragmenting system ... Both the excitation energy and the expansion energy increase with the incident energy for a given system. At a given excitation energy per nucleon, an increase of the mass of the system leads to identical distributions for the size of the fragments whereas their multiplicity scales as the available charge. This behaviour is expected in particular if multifragmentation originates in the spinodal decomposition of a finite piece of nuclear matter.

1 Introduction

The decay of highly excited nuclear matter through multifragmentation (emission of several fragments in a short time-scale) is one of the most studied subjects at the present time. Whether this process finds its origin in the dynamics of nuclear collisions, or is simply the normal decay mode of hot nuclear matter is still largely debated. Various theoretical approaches have been proposed which reflect this ambiguity, which can be classified as statistical type models, sequential binary decays, or dynamical simulations leading to spinodal decomposition of nuclear matter. Simultaneously, with the advent of powerful 4π devices, which are absolutely necessary to improve the experimental knowledge of this process, numerous experimental results have appeared; some of their conclusions appear however as contradictory, eventually because of the difficulty of clearly defining the system which undergoes multifragmentation. In this paper we will briefly remind some of the features of multifragmentation predicted by models of different classes. Then results concerning heavy systems studied with INDRA will be presented, with the observed variations with the incident energy and the total mass of the system. The scaling observed in this last case may give a first indication that multifragmentation finds its origin in the spinodal decomposition of a finite piece of nuclear matter.

2 A brief glance at some models for multifragmentation

2.1 Statistical type models

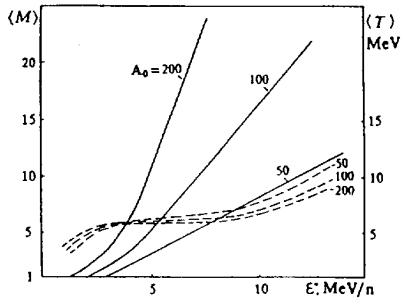

Figure 1: *Average multiplicity of clusters (solid curves) versus the excitation energy of the decaying system. From* [2].

When nuclei are given excitation energies equal to their binding energies, their very existence become questionable, and they were assumed to explode into multiple fragments of different masses. The very name "multifragmentation" was attributed to this process in the framework of a statistical type model, which followed the disintegration modes of a nucleus when it is heated more and more [1]. Since then several versions of such models have flourished, see for instance references [2-4].

The basic hypotheses are i) that the system is in thermodynamical equilibrium at break-up, with some precautions for chemical equilibrium, which is assumed to be verified on an ensemble of events, and not on an event-by-event basis.

ii) that at sufficiently high energy the probabilities of finding different partitions are mainly determined by their statistical weights, with negligible influence of the preceding dynamics. In such a framework, (we will take as an example the SMM

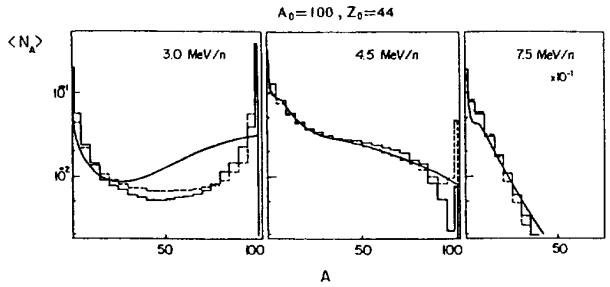

Figure 2: *Average multiplicity of clusters versus the mass. From* [2].

model [2]), the evolution of the deexcitation of a nuclear system is sketched in figures 1 and 2; the first one shows the average cluster multiplicity versus the excitation energy. Below 2-3 AMeV one can recognize the usual compound nucleus in the single existing fragment. Multifragmentation (at least 3 fragments) sets-in around 3 AMeV slightly earlier for heavy systems than for lighter ones. The finite number of nucleons, correlated with the increasing number of fragments leads to the evolution of the mass distribution from a U-shape (evaporation) to an exponential shape, passing through a very broad distribution around 4-5 AMeV . Note that a power law, presented in some papers as a proof of multifragmentation, and even of a phase transition, is never observed in such a description. Several parameters enter these models, among which of course the initial size and excitation energy of the system which must be fixed when comparing to experimental data. Two specific volumes also have to be parameterised, one governing the barrier against multifragment configurations, the second being the break-up (freeze-out) volume corresponding to the vanishing of nuclear forces. The latter is at least three times the volume of a cold nucleus of equal mass, which is the minimum volume required to put spherical fragments in a spherical volume without letting them overlap. In the more recent versions, and for matching with experimental data, the possibility of giving an extra radial energy to the fragments was included, which indicates that the dynamics can not be completely neglected. Therefore the energy of fragments could be reproduced by playing with the density of the system (i.e. kinetic Coulomb energy)

and this radial energy [5]. In order to reproduce experimental data for central collisions, the multifragmenting system must be much lighter and less excited than allowed by the nuclear collision, and be quite dilute. It is thus justified to wonder how such a configuration can be reached during the collision, and even if it can be attained.

2.2 Sequential evaporation from an expanding source

It was pointed out by W. Friedman some years ago that "multifragmentation" can arise from the sequential decay of a hot source [6]. In his "expanding evaporating source" model, the entropy of the source is supposed to be frozen at normal density. Then its cooling by particle evaporation at constant entropy naturally induces an expansion process. For moderate initial temperatures ($\leq$ 12 MeV) the system gently goes back to normal density (see fig. 3). At higher temperatures, during the course of its expansion,

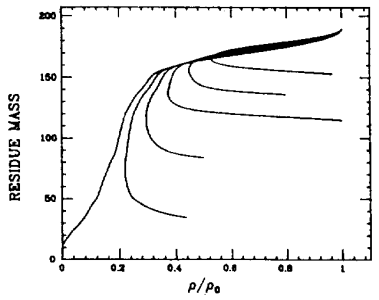

Figure 3: *Instantaneous mass as a function of the instantaneous density, calculated during the evolution of* ^{197}Au *starting from temperatures of 10 to 15 MeV in 1 MeV steps. From* [6].

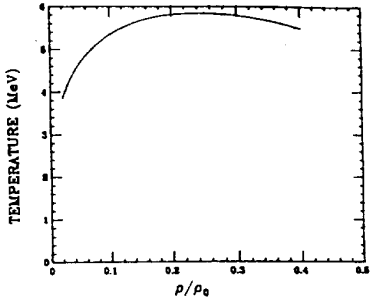

Figure 4: *Locus of conditions where fragment emission takes place. From* [6].

the system may encounter the force freeze-out condition (corresponding to a vanishing of the nuclear interaction) and emit successively, but in a very short time, several fragments. This process occurs at low density, and at a rougly constant temperature of $\sim$ 5-6 MeV, as shown in fig. 3,4. It will be shown later that in the energy domain under consideration here, the expansion energy so generated remains small.

2.3 Dynamical simulations

Dynamical simulations (Landau-Vlasov, BUU, BNV ...) have proven quite successful in predicting the evolution of colliding nuclei, provided that their basic ingredients

are constrained by confrontation with experimental data [7]. It has been known for a long time that during the first instants of a collision the system suffers a compression whose strength depends on the violence of the collision (incident energy and impact parameter). For central collisions at moderate energies the system induces a monopolar type oscillation, while for higher energies it enters an expansion phase and never comes back to normal density as shown in fig. 5 [8]. Most of the models predict that

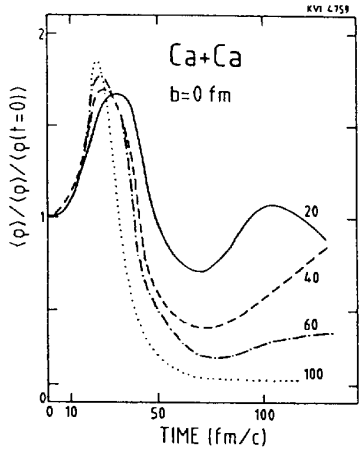

Figure 5: *Average density versus time for central collisions between Ca nuclei, at different incident energies. From* [8].

a highly unstable region of the nuclear equation of state is then explored (spinodal zone). For heavy systems, some exotic configurations emerge from calculations, such as the bubbles, toroids ... depicted in fig. 6, 7 [9, 10]. It seems clear that if the system stays in the spinodal region long enough to let instabilities develop, it will end up by multifragmenting. Deep enough in the spinodal zone, volume instabilities are probably preponderant; when a bubble or a toroid is formed, one may also evoke surface instabilities of Rayleigh type [11]. Finally for very heavy systems, it is natural to think of the role of Coulomb instabilities [12]. None of these dynamical simulations is able to correctly follow the evolution of a nuclear system in the spinodal region, simply because they neglect correlations and fluctuations. It was suggested some years ago that these effects could be simulated by introducing a stochastic term in transport equations, analogous to a Langevin force [13, 14].

2.4 *Spinodal decomposition of finite nuclei*

Recently, a detailed study of the development of instabilities, and of spinodal decomposition of finite nuclei was undertaken [15–17]. Let us just briefly recall some findings

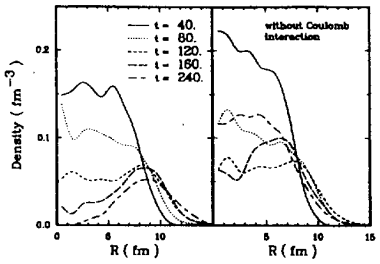

Figure 6: *Evolution of the average density versus the distance from center, at different times, for the Gd+U system at 35 AMeV and b=3 fm. From* [10].

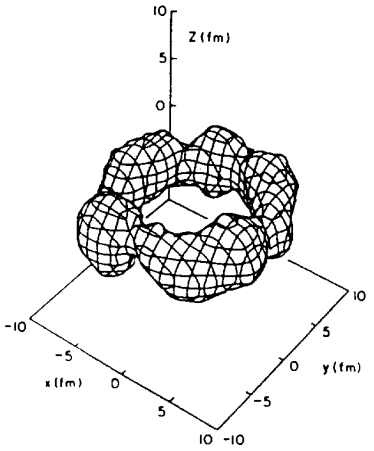

Figure 7: *Surface of constant nucleon number density ($0.3\rho_0$) for a 60 AMeV Nb+Nb central collision at t=160 fm/c. From* [9].

directly connected to experimental observables: the most unstable modes have characteristic times, τ, of about 40 fm/c, corresponding to wavelengths of 10 fm. Consequently the partitions in fragments of equal size are favoured, with a typical charge Z$\sim$10. An increase of the total mass of the system results in a larger number of fragments, without changing their size. The time necessary for complete clusterization is about $3-4\times\tau$, or 120-150 fm/c. Due to the most favoured wavelengths, fragments are formed at the surface of the system, with a depletion at the centre, as shown in fig. 8a. Surface effects, and also the beating of different modes may induce the coalescence of two prefragments during the clusterization phase (fig. 8b), which accounts for the presence of some rare much heavier primary fragments (see further fig. 22). It was observed however that this coalescence process is counterbalanced by Coulomb and radial expansion effects, and therefore should only play a role at moderate energies for heavy systems. If both these effects are important, the system expands quickly without time to develop fluctuations, and may therefore directly induce a vaporization stage.

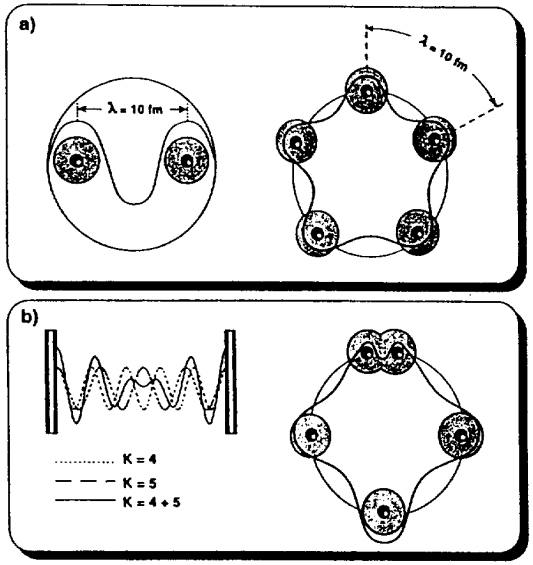

Figure 8: *Simplified picture of the process of clusterization for a nuclear system inside the instability region corresponding to the development of the most unstable modes (a) and to the beating of two different modes (b). From* [15].

3 Heavy systems studied with INDRA

3.1 INDRA

The experimental data presented in this paper were obtained with the 4π multidetector INDRA, operating at the GANIL accelerator. Mainly designed to study nuclear collisions in which rather large numbers of fragments ($\sim$ 10) and light charged particles ($\sim$ 40) are produced, INDRA is characterised by its large geometrical coverage, $\sim$ 90% of the 4π solid angle, fragmented in 336 detection modules [18]. Low energy identification thresholds and large energy ranges were obtained through the design of three-layer telescopes, composed of an axial-field ionization chamber operated at 30 mbars of C_3F_8, a 300 μm silicon detector and a CsI(Tl) scintillator, thick enough to stop all emitted particles, coupled to a phototube. Such a telescope can detect and identify from protons between 1 and 200 MeV to uranium ions of 4 GeV. Past 45 ° where fast projectile-like fragments are no longer expected, the telescopes comprise

only two stages, the ionization chamber operated at 20 mbars and the scintillator. Finally the very forward angles (2-3 °) are occupied by Ne102-Ne115 phoswiches. Charge resolution of one unit was obtained up to Z=54 for the fragments identified through the $\Delta E - E$ method in the Si-CsI couple, and up to Z=20 when the ΔE signal is furnished by the ionization chamber. Identification thresholds increase from $\sim$ 0.7 AMeV for Z=3 to $\sim$ 1.7 AMeV for Z=50. Nuclei with lower energies can be detected, but not correctly identified, and will not be considered in the following.

3.2 The studied systems

A series of systems were studied with the INDRA device in order to follow the properties of multifragmentation when varying the size of the system, the beam energy, or the initial asymmetry [19]. Among them we will mention here the $^{36}Ar+^{58}Ni$ and $^{129}Xe+^{nat}Sn$ system between 32 and 50 AMeV and the $^{155}Gd+^{238}U$ system at 36 AMeV . Thus one has at hand systems with total masses evolving from $\sim$100 to $\sim$400, in an (available) excitation energy range between 7 and 12 AMeV . The Ar, Xe and Gd beams were delivered by the GANIL cyclotrons, with intensities kept below 5×10^7pps in order to avoid pile-up, especially in the zone of the rare high multiplicity events. The target thicknesses were about 100-200 $\mu g/cm^2$, which allows slow fragments to escape from the target. A minimum bias trigger based on the multiplicity was used in all cases, events were registered if at least 4 modules had fired; this value was increased to 8 for the $^{155}Gd +^{238} U$ system, to minimise the proportion of events due to reactions with the 45 $\mu g/cm^2$ carbon backing of the uranium target.

3.3 Search for the multifragmenting source: selection of events

One of the first experimental facts which was confirmed by the INDRA data is the overwhelming dominance of dissipative binary collisions in the reaction cross section at energies between 30 and 100 AMeV and whatever the masses of the colliding partners [20, 21–25]. Most of these reactions are however not purely binary as they are accompanied by preequilibrium or non-equilibrium emissions (forward peaked Fermi jets, mid-rapidity emission ...) [20, 26–33]. The occurrence of a phenomenon which can be assimilated to incomplete fusion, because a transient system containing a major fraction of all incident nucleons can be characterised, remains marginal, as it concerns less than 1% of the reaction cross section. Its study is however essential, as it may be the only case where a multifragmenting system can be clearly isolated and its properties characterised, as opposed to the "binary reactions" where the separation of the two entities from each other and from the eventual mid-rapidity emission is difficult at the energies under consideration here. Isolating "fused systems" is also the only way of obtaining very heavy systems containing more than 250 nucleons.

The detailed procedure followed to isolate these rare events, and the motivations for doing so, are explained in another contribution to this meeting [34]. We will simply recall here that we require the detection of a significant fraction (80%) of the total charge, and of 80% of the initial linear momentum (constructed with the charge instead of the mass). Being interested in the multifragmentation process, the detection of at least three fragments with charge $Z \geq 5$ is required (this minimum charge is sometimes lowered to 3, without changing the behaviour of our observables). Finally the preferred direction of emission of matter in the centre of mass of the reaction (flow angle) is determined from the calculation of the energy tensor of the fragments[35], and the requirement is made that this angle be larger than 60° . Indeed, when one builds a diagram resembling the well-known "Wilczynski plot" for low energy deep inelastic collisions, it is observed that the system has no time to rotate for peripheral and mid-central collisions, as long as the maximum of energy dissipation is not reached [35, 36]. It is only when this limit is attained that all flow angles are populated. Even in this case of maximum dissipation, the angular distribution remains highly anisotropic, except for flow angles larger than 60° . An isotropic flow angle distribution is expected if a "fused" system has been formed, which emits fragments isotropically, and therefore has no reason to remember any privileged direction with respect to the beam axis. Thus the idea underlying the chosen selection is that while a fused system should be present at all flow angles, binary collisions should vanish when this angle is large, giving way to an almost pure phenomenon. This idea is supported by dynamical simulations, as

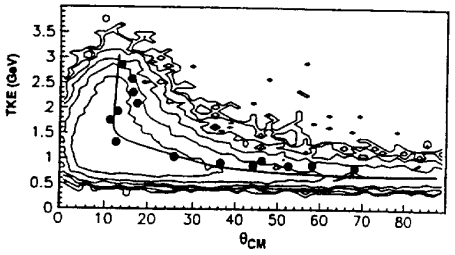

Figure 9: *Comparison between the generalised Wilczynski diagram for a fragment multiplicity $M_f > 3$ and theoretical results (dots) obtained from different simulations at different impact parameters. From* [37].

shown in fig. 9, extracted from [37], which exhibits the trajectory of the system on the "Wilczynski diagram": the points corresponding to θ_{CM} lower than 30° correspond to binary outgoing channels, while all the other ones result from several simulations for central collisions (b=2 fm, with different random number generator seed); in this case a fused system is obtained, and the variations of the calculated flow angle just reflect that any value is equally probable.

To summarize, the selection performed to isolate events resulting from the multifragmentation of a fused system (single source) reads:

$\sum Z_{det} \geq 0.8 \times (Z_{proj} + Z_{targ})$; $\sum ZV_{det} \geq 0.8 \times (ZV_{proj})$; $Mult_{Z\geq 5} \geq 3$; $\theta_{flow} \geq 60°$.

4 Evolution of experimental data with the incident energy and the total mass of the system

4.1 Multiplicities

The multiplicity distributions measured for the $^{129}Xe + ^{nat}Sn$ system at four incident energies are shown in fig. 10 [38]. The average value of the total multiplicity of charged products as well as that of the fragment multiplicity increases with incident energy, while the width of the distributions remain roughly constant. The increase is more

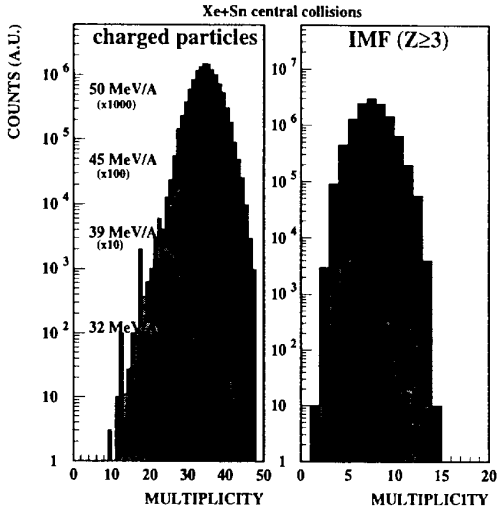

Figure 10: *Evolution of multiplicity distributions with incident energy for the $^{129}Xe + ^{nat}Sn$ system.*

pronounced for the total multiplicity (therefore for the light charged particles) than for the fragments. The larger number of fragments and particles reflects the augmentation of the excitation energy of the system at break-up with the warning that more light charged particles may also indicate an increase of preequilibrium emission, which would conversely limit the increase of excitation energy of the system. The larger number of fragments is obviously connected with a decrease of their size, as the charge distribution drops by a factor 100 between Z=3 and Z=38 (Z=22) at 32 (50) AMeV [39]. When

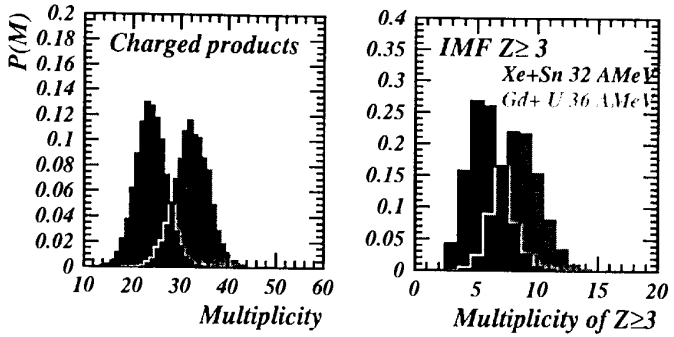

Figure 11: *Evolution of multiplicity distributions with the mass of the system.*

comparing now the data for two systems with different masses (fig. 11), but the same available energy per nucleon ($\sim$ 7 MeV), a strong increase of the multiplicities is also observed when going from $^{129}Xe+^{nat}Sn$ (248 nucleons) to $^{155}Gd+^{238}U$ (393 nucleons). The increase of the number of fragments scales as the total charge of the systems, being multiplied by $\sim$1.5. The total multiplicity shows a smaller increase, simply because of the relatively larger number of composite particles as compared to protons emitted by the heavier system.

4.2 Fragment kinetic energies

Some insight into the dynamics of the reaction can be obtained by looking at the kinetic energies of the fragments as a function of their charge; indeed, the fragment kinetic energies, in their emitter frame, are assumed to comprise two parts in addition to the kinetic Coulomb energy, one coming from the thermal energy of the emitter, and the other one from collective effects such as an eventual expansion energy. The thermal part should be independent of the size of the fragment, whereas the collective part is expected to increase proportionally to the fragment mass. Some examples of this evolution are shown in fig. 12; in all cases, it was assumed that the reference frame of the emitter was the reaction centre of mass. This is a straightforward assumption for the quasi symmetric system $^{129}Xe+^{nat}Sn$. It is more questionable for the asymmetric system $^{155}Gd+^{238}U$ but is supported by the finding that for this system and for $^{129}Xe+^{nat}Sn$ at 32 AMeV the reconstructed velocity of the system formed with all measured fragments ($Z \geq 5$) was similar, namely 6% higher than the centre of mass velocity. Moreover the energy of the fragments is independent of their emission angle.

The evolution of the average kinetic energy with Z is the same for all systems, namely a "rise and fall" behaviour when Z increases. The falling part is only due to the heaviest fragment in each partition, as can be seen in the right part of fig. 12

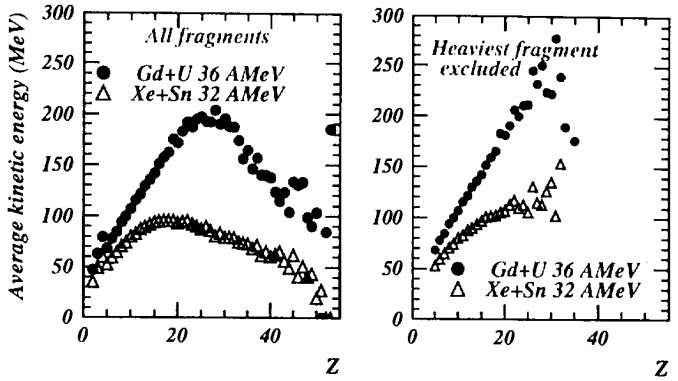

Figure 12: *Experimental average kinetic energy of the fragments, in the emitter frame, versus their charge for the 36 AMeV $^{155}Gd+^{238}U$ and 32 AMeV $^{129}Xe+^{nat}Sn$ systems*

where a continuous rise of the kinetic energy appears if this fragment is not included. Obviously, one is not dealing with a solely thermal origin of the fragment energy. Some collective effect has to be present, although part of the variation has to be attributed to Coulomb repulsion. This last effect is probably at the origin of the huge difference of kinetic energies for a given Z when going from the $^{129}Xe+^{nat}Sn$ to the $^{155}Gd+^{238}U$ system. But for the former differences are also observed when the incident energy is increased. For instance for Z=10, a mean kinetic energy of 80 MeV is measured at 32 AMeV, while it is $\sim$100 MeV at 50 AMeV [40]. This pleads for the existence of a collective expansion energy.

4.3 Simulation of multifragmentation with an event generator

In order to determine in a consistent way the radial expansion energies, we use for all systems the event generator SIMON [41]. One of the initial configurations of this code is a hot nuclear system which has just exploded in a given number of excited fragments. The initial mass, charge and excitation energy $(A_0, Z_0, \varepsilon_0)$ of the initial system are given as input, as well as the number of primary fragments. The mass of each fragment is chosen randomly between a given minimum value A_{min} and A_0. In the following, A_{min} was set to 20. The geometrical arrangement of the fragments can be specified, and two possibilities were considered: firstly a compact configuration, with fragments at the corners and face-centres of a pyramid; the distance between the centres of two fragments is minimised to the sum of their radii plus 2 fm, to simulate a freeze-out configuration where nuclear forces have vanished. The density of the system is then approximately $\rho_0/3$ [42], for the reason already quoted in Sect 2.1. The second

configuration consists in placing the heaviest fragment at the centre, and the others around it. In this case the additional 2 fm are suppressed, as the distances between fragments are already somewhat larger than in the previous one. Part of the excitation

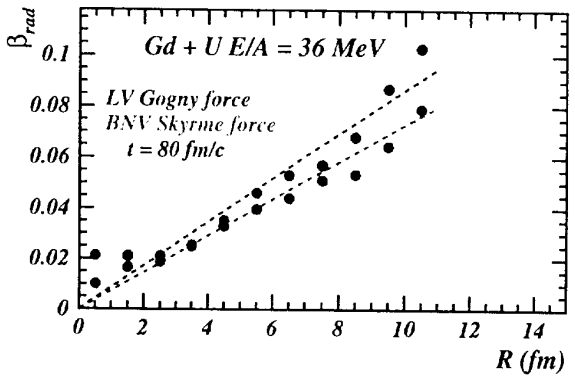

Figure 13: *Radial velocity of the pseudo-particles versus their distance from the centre, calculated for the 36 AMeV $^{155}Gd + ^{238}U$ system within a Landau-Vlasov and a BNV simulation.*

energy can be taken as expansion energy. Then, besides that due to thermal motion and Coulomb forces, each fragment receives an additional velocity depending on its position with respect to the centre of mass (r_F): $v = v_0 \times r_F/R$, with $R^2 = < \sum r_F^2 >$. The expansion energy per nucleon quoted in the following is $\varepsilon_{rad} = 0.5 m_0 v_0^2$ (m_0 is the nucleon mass). The fragments start flying apart, and they are allowed to deexcite with probabilities given by the transition state model [43]. The trajectories of all particles present at each time step are then followed, which insures the preservation of space-time correlations. As defined here, the radial expansion energy is said to be self-similar, and this type of variation is implemented in most of the event generators used in the field [44]. We wondered whether there was some physical reason for this behaviour, and we then turned to dynamical simulations of nuclear reactions. In fig. 13 is plotted the average radial velocity of particles versus their distance to the centre, obtained in the framewok of two simulations, at a time just preceding the formation of fragments [45, 46]. The evolution of the radial velocity versus the distance is compatible with a linear dependence, which supports the hypothesis of self-similarity assumed in event generators.

Results of the simulation are shown in fig. 14 to 17. They were filtered through the detector acceptance. It was required that not only the fragment kinetic energies agree with experimental data, but also other variables such as the multiplicities, the charge

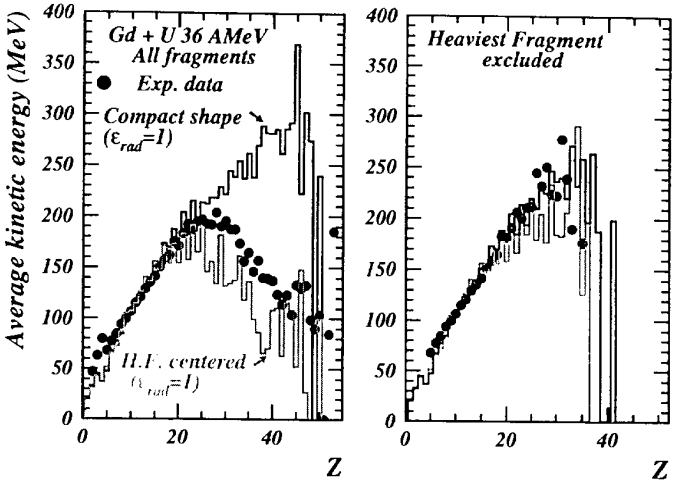

Figure 14: *Comparison of experimental fragment energies with SIMON simulations, for the 36 AMeV $^{155}Gd + ^{238}U$ system. Two geometrical configurations were used, a compact shape, and the other with the heaviest fragment located close to the centre.*

distributions, the size of the largest fragments... In the examples shown here, the total system, with all the available excitation energy was used as input. We are aware that preequilibrium emission is probably present, but we feel that the time scale for this emission is the same as that for "deciding" to evolve towards multifragmentation. Therefore the exact instant of particle emission - just before or just after the break-up - should not be of crucial importance, and Coulomb effects are alike. For the two systems, $^{129}Xe + ^{nat}Sn$ at 32 AMeV and $^{155}Gd + ^{238}U$ at 36 AMeV the results are similar: an excellent agreement is obtained between data and simulation for all variables shown in fig, 15 and 17, provided an expansion energy of 0.5 (1.0) AMeV for $^{129}Xe + ^{nat}Sn$ ($^{155}Gd + ^{238}U$) is assumed. In more detail one can however note that while the charge of the heaviest fragment is well predicted, those of the second and third largest are overestimated by the simulation. It is shown by R. Bougault in this meeting [47] that an almost perfect agreement on all these variables is obtained when performing a simulation of the $^{129}Xe + ^{nat}Sn$ system with the SMM model, although starting from a very different initial multifragmenting system (A_0, Z_0, ε_0 are all smaller); the expansion energy is however the same, 0.5 AMeV .

It appears in fig. 14 that the rising part of the E(Z) curve is very well reproduced by the simulation; in order to correctly get the falling part, a special geometry of the system has to be chosen: while for the compact shape described earlier the kinetic energy

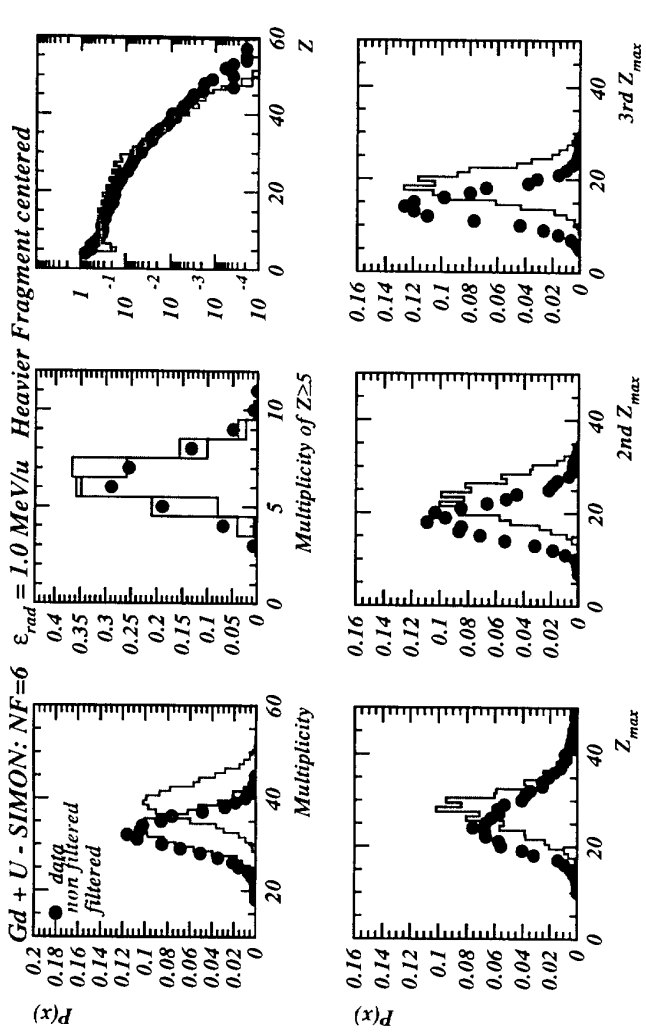

Figure 15: *Comparison of experimental data with SIMON simulations, for the 36 AMeV $^{155}Gd + ^{238}U$ system. In P(x), x stands for the variable in abscissa.*

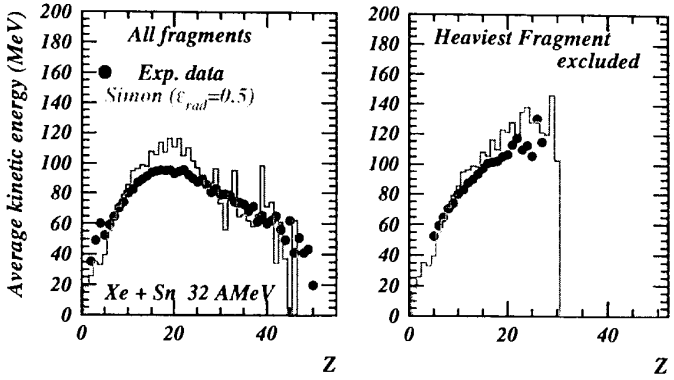

Figure 16: *Comparison of experimental fragment energies with SIMON simulations, for the 32 AMeV $^{129}Xe + ^{nat}Sn$ system. The geometrical configuration is that with the heaviest fragment located close to the centre.*

is continuously increasing with Z, a correct overall behaviour is obtained if the heaviest fragment is located at the centre of the system; this is immediatly understandable as Coulomb effects from other fragments mutually cancel each other, and the radial energy is minimised. This is also in agreement with a density profile of the system which has a smooth descent at large radius. However we will show in the last section that low energies of the heavy fragments can be associated with dynamical, and not geometrical, reasons.

5 Expansion energy near the threshold

Radial expansion energy can follow from a compression phase at the beginning of the nuclear collision (dynamics), or simply be due to the thermal pressure existing as soon as a nucleus is sufficiently heated and decays at constant entropy. We tried to make a choice between these assumptions by looking at a systematics of some results corresponding to the onset of radial expansion energy. It should be noted that the value of the expansion that we obtain with the help of the event generator is free from Coulomb energy. We were able to determine the expansion energy of the multifragmenting system for $^{155}Gd + ^{238}U$, $^{129}Xe + ^{nat}Sn$ between 32 and 50 AMeV (although the data at 39 and 45 are not as fully analysed as the others); to enlarge the explored mass domain, we also searched for a single multifragmenting source in the 52 AMeV $^{36}Ar + ^{58}Ni$ reaction, just by applying the selection defined in sect. 3 [48] (with, obviously, the minimum charge for fragments reduced to 3). The result found is that there is no expansion; we have included this result in the systematics presented in this section,

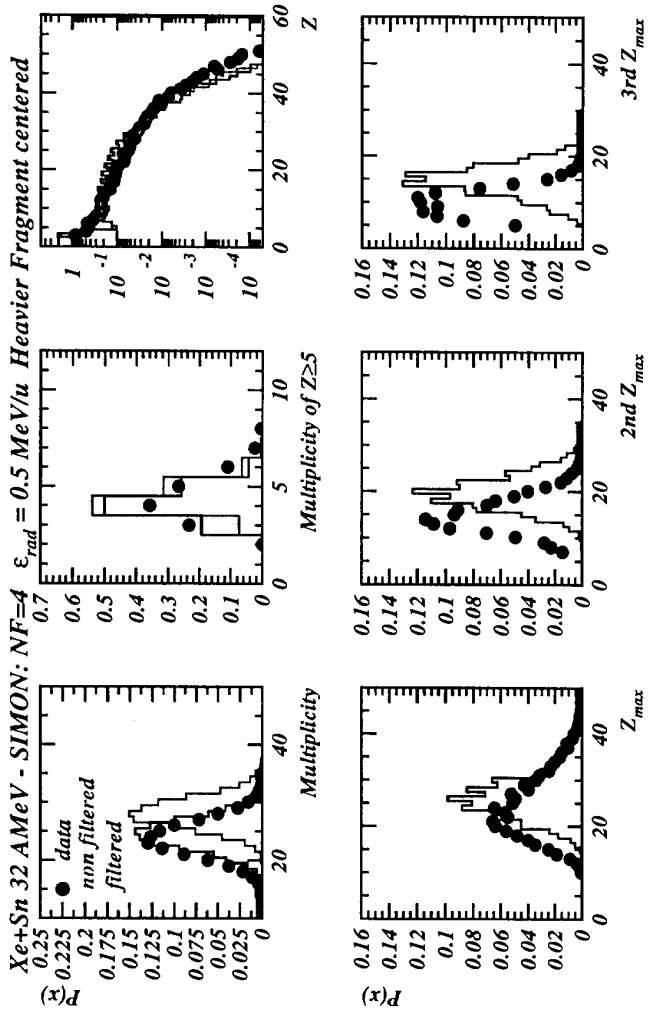

Figure 17: *Comparison of experimental data with SIMON simulations, for the 32 AMeV $^{129}Xe + ^{nat}Sn$ system. In P(x), x stands for the variable in abscissa.*

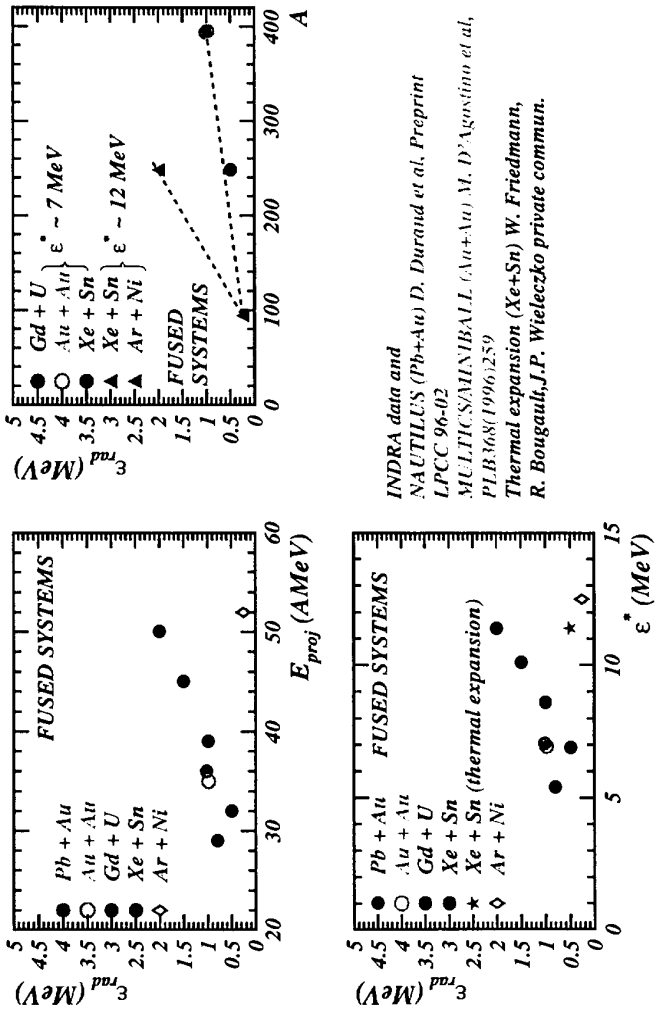

Figure 18: *Radial collective energy per nucleon ε_{rad} as a function of (a) projectile energy, (b) excitation energy per nucleon ε^* of the single source, (c) total size of the system for different ε^*; the lines are to guide the eye.*

as we feel that even if some binary events remain in the selection, it can only increase the expansion energy. Many data on expansion energy have been published in this domain of incident energy, where expansion starts to appear. In fig. 18 we voluntarily restrict to: firstly the INDRA data, which result from a single series of measurements (and therefore a single set of calibrations), selecting a single multifragmenting source in the same way and extracting the expansion energy with the same event generator. We added a result from the Nautilus collaboration [50], which fulfill the last two conditions, and another one from the MULTICS/MINIBALL collaboration [44], obtained from a code similar to SIMON. The values of the expansion energy are first plotted versus the beam energy, which allows us to deduce that expansion begins to appear in nuclear collisions above ~25 AMeV for sufficiently heavy systems. When plotted versus the total available excitation energy, the behaviour is the same, with a threshold near 4-5 AMeV . A calculation using the expanding evaporating source was performed, corresponding to the $^{129}Xe+^{nat}Sn$ system at 50 AMeV . The expansion energy arising from thermal expansion found in this case is 0.5 AMeV(star in fig. 18)[49], to be compared to the experimental value of 2 AMeV . This indicates that the expansion energy that we observe mainly results from a compression of the system. Finally, in this plot, one can notice three groups of points, $^{36}Ar+^{58}Ni$, $^{129}Xe+^{nat}Sn$, and the three very heavy systems. This led to the idea to plot the expansion energy versus the total mass of the system, for two values of the available excitation energy [51]. It thus appear that for a given ε^* the radial expansion energy increases with the mass of the system, but also that a minimum mass (~100) would be required for inducing expansion. This again is in favour of a compression phase followed by expansion, which is expected to be stronger for heavier systems.

6 Scaling law with the mass of the system: spinodal decomposition of nuclear matter?

Among the studied reactions, the 32 AMeV $^{129}Xe+^{nat}Sn$ and the 36 AMeV $^{155}Gd+^{238}U$ lead to "fused systems" with the same excitation energy per nucleon ($\varepsilon^* = (1/A_{tot}) \times (E_{cm}+Q)$), around 7 AMeV . We have already stressed in section 4 that the multiplicities of fragments scaled as the total charges of the systems, as is recalled in the right part of fig. 19. The charge distributions, on the other hand, are perfectly superimposable, over three orders of magnitude. In more detail, the sizes of the largest fragment are identical for the two systems, while that of the second and third largest are on average smaller by 5 units for the $^{129}Xe+^{nat}Sn$ system (see fig. 15,17). This experimental finding of equal size fragments with different multiplicities recalls immediately the predictions of multifragmentation related to the spinodal decomposition of finite nuclei (see Sect 2.4). Therefore calculations were performed for these two reactions, to test whether the theoretical predictions would match the experimental results. We

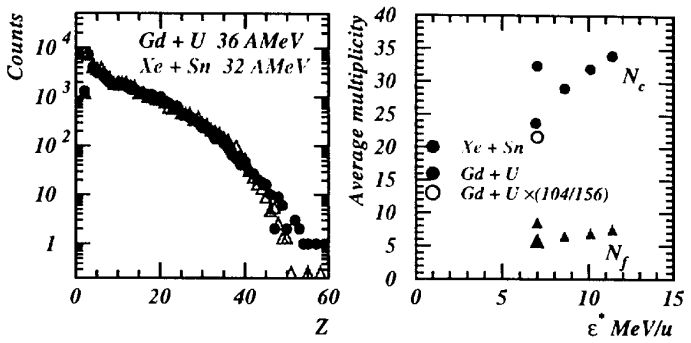

Figure 19: *Comparison of the experimental charge distributions (left), and average multiplicities(right) of charged products (N_c) and of fragments (N_f) for the 36 AMeV $^{155}Gd+^{238}U$ and 32 AMeV $^{129}Xe+^{nat}Sn$ systems. On the right part of the figure close symbols refer to the measured values, while the open symbols are the scaled multiplicities for $^{155}Gd+^{238}U$.*

recall the principle of this type of calculation, which follows the progress of the system during the nuclear collisions and up to the cold measurable particles. During the first part, the evolution of the density distribution function is followed thanks to a BNV simulation; the mean field is approximated by a Skyrme force applied to a folded density to simulate the finite range of the nuclear force [16]. The collision integral is calculated from [52], with a constant nucleon-nucleon cross section of 41 mb. During the first 100 fm/c, the fluctuations were shown to be sufficiently small to be neglected. This is no longer the case at later times, as the system enters the spinodal zone of high mechanical instabilities. Thus at that time a stochastic mean field simulation (SMF) is grafted on, with the mass, charge, temperature and radial velocity of the system as given by BNV. This part of the simulation is pursued for 200 fm/c, to allow for fragment formation. Finally, as the fragments still bear some excitation energy, their configuration at the end of the SMF calculation is given as input to the SIMON code, until full deexcitation.

The results for the $^{155}Gd+^{238}U$ system are shown in fig. 20, for the same set of variables already presented apart from the total multiplicity. An excellent agreement between experiment and calculation is observed for the fragment multiplicity, the charge distribution and the sizes of the three largest fragments. When decreasing the mass of the system, the experimental conclusions hold for the results of calculations: the charge distribution does not change while the fragment multiplicity decreases, see fig. 21. In the framework of this model, one might thus state that spinodal decompo-

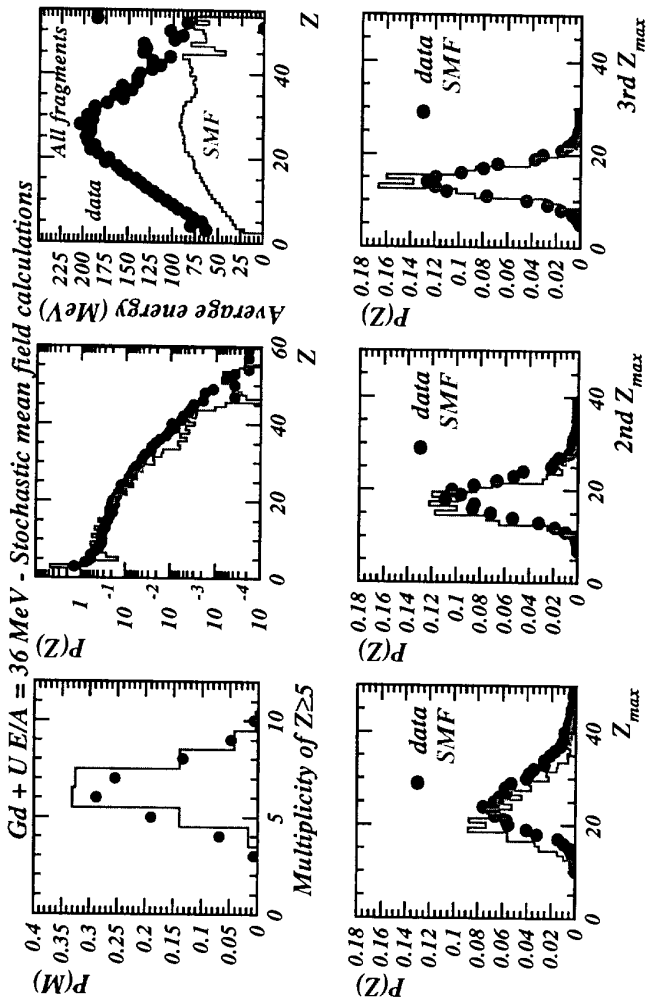

Figure 20: *Comparison of experimental data (points) with the results of the stochastic mean field simulation (histograms), for different observables of the $^{155}Gd+^{238}U$ system.*

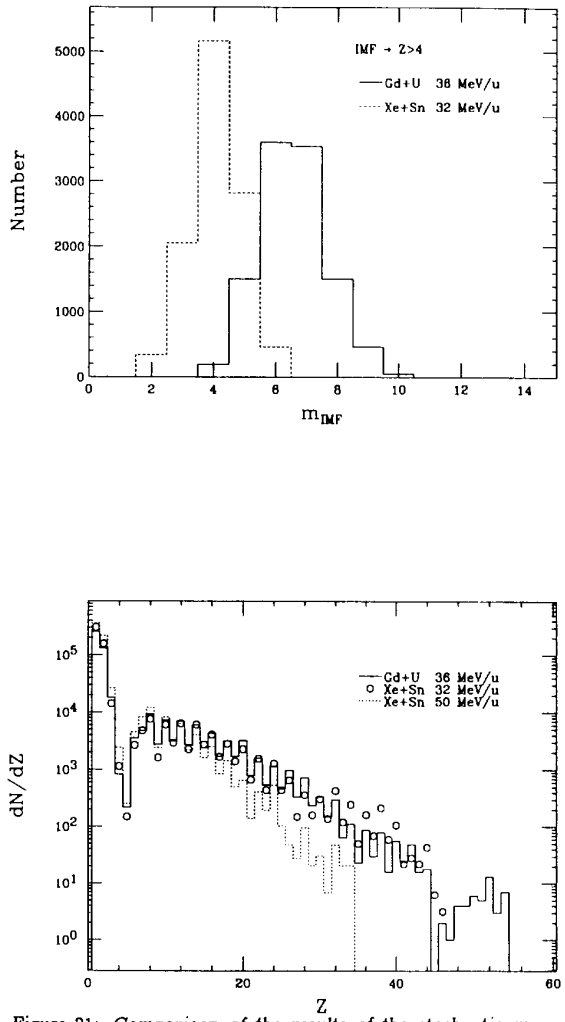

Figure 21: *Comparison of the results of the stochastic mean field simulation for the systems 32 AMeV $^{129}Xe+^{nat}Sn$ and 36 AMeV $^{155}Gd+^{238}U$. Also shown is the calculated charge distribution for $^{129}Xe+^{nat}Sn$ at 50 AMeV extracted from [53].*

sition of a finite system can be the origin of the observed multifragmentation process. There is however a disappointing drawback in this "complete model", namely the fragment kinetic energies. Indeed the dynamics is fully included in this type of simulation, and therefore all effects such as thermal energy, Coulomb repulsion and expansion following the compression phase should naturally add to give the correct fragment energy . The calculated evolution of the fragment energy with their charge resembles the experimental one: the rise-and-fall behaviour naturally appears, due to the origin of the heavier fragments; indeed the coalescence of two nascent fragments slows them down. But the absolute value of the calculated energy is too low, as can be seen in fig. 20; this is a general trend of this ensemble of simulations [16, 53], which may arise from an incorrect variation of the surface energy with the density. This point should be clarified before definite conclusions on the origin of multifragmentation can be drawn.

6.1 Remarks on the link between initial and final partitions

It was shown in section 4 that a good reproduction of the properties of the multifragmenting systems was obtained in the framework of the SIMON code. But similar conclusions are drawn from comparisons of data with the SMM, or with a dynamical simulation. Therefore it appears that the same final fragment distributions can be obtained starting from very different initial partitions at break-up. Let us be more quantitative:

i) in the case of the 32 AMeV $^{129}Xe +^{nat} Sn$ system and using SIMON, we got satisfactory results for multiplicities, charge distributions, size of the heaviest fragments. Initial conditions were then: $A_0 = 248, Z_0 = 104, \varepsilon_0^* = 6.9MeV, \varepsilon_{rad} = 0.5MeV$ (ε_0^* includes ε_{rad}); the initial average fragment charge is $< Z_F >= 26$. A consistent inclusion of some preequilibrium light particle emission led to exactly identical final distributions with $A_0 = 215, Z_0 = 90, \varepsilon_0^* = 6.1MeV, \varepsilon_{rad} = 0.5MeV$ and $< Z_F >= 22.5$ [54]; the assumed multiplicity of (removed) preequilibrium particles is in agreement with the difference between the measured and calculated mean values.

ii) from the SMM simulation [47], an even better agreement with the same experimental quantities is obtained for $Z_0 = 83, \varepsilon_0^* = 5.5MeV, \varepsilon_{rad} = 0.5MeV$; the break-up density is $\rho_0/3$, as in i). The initial charge distribution has not yet been looked at.

iii) For Gd+U, initial values input in SIMON may be either $A_0 = 393, Z_0 = 156, \varepsilon_0^* = 7.1MeV, \varepsilon_{rad} = 1.0MeV$ and $< Z_F >= 26$ (as shown in fig. 22), or with 15% (in mass) of preequilibrium removal $A_0 = 334, Z_0 = 133, \varepsilon_0^* = 5.85MeV, \varepsilon_{rad} = 1.0MeV$ and $< Z_F >= 22$. Note that, as in i), a 15% change of the initial mass (charge) is not sufficient to modify the extracted expansion energy. From spinodal decomposition, one gets, when the system enters the unstable region, $A_0 = 360, Z_0 = 142, T = 4MeV, \varepsilon_{rad} = 3.4MeV$. Note that here the radial energy is that of pseudo-particles, as plotted in fig. 13, i.e. before the break-up of the system into fragments; it is found

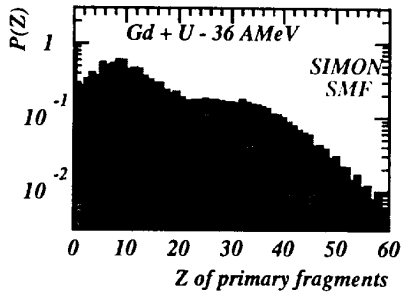

Figure 22: *Initial fragment charge distributions from SIMON, and from the stochastic mean field simulation, for the $^{155}Gd +^{238} U$ system.*

to be much lower at the end of the clusterization phase. Also, at this time only 108 charges remain bound in fragments (with $< Z_F >\sim 11$ - see fig. 22): as expected light particles are continuously leaking out of the system during all the reaction phases.

We are then faced with very different initial conditions (especially the fragment size distributions) which all converge to the same final observables: we are forced to recognize that the present data can not assess whether multifragmentation is mainly governed by dynamics and volume instabilities or simply by statistical phase space considerations, eventually flavoured with reducibility and thermal scaling [55].

7 Conclusions

With the birth of a powerful 4π multidetector, we were able to evidence and characterise the multifragmentation of a single piece of nuclear matter, comprising essentially all the nucleons (≥ 200) of two colliding heavy nuclei. The rise of the incident energy increases the energy deposited in this system, as indicated by the charged particle multiplicity. Besides the usual Coulomb and thermal terms, an extra collective energy has to be assumed to account for the fragment kinetic energies; this radial energy is shown to follow from a compression stage during the collision rather than originating simply from thermal pressure. It shows up from 25 AMeV incident energy, and in systems with a sufficiently large mass (100 nucleons). All the experimental features are well reproduced by several statistical models for multifragmentation, although they start from different configurations.

Scaling laws were found when increasing the total mass of the system, which result in a scaled number of identical fragments, provided however that the system is large enough. This would have been taken as a first hint that multifragmentation originates in the spinodal decomposition of nuclei, as predicted by recent simulations which include the dynamics of the collision and the multifragmentation stage; an underestimation of the fragment kinetic energy was however found, which demands for

refinements in the basic ingredients of the dynamical simulation.

References

1. J.P. Bondorf, Journal de Physique **37-C5** (1976) 195.
2. J.P. Bondorf et al, Phys. Reports **257** (1995) 133.
3. J.A. Lopez and J. Randrup, Nucl. Phys. **A503** (1989) 183; **A512** (1990) 345 and preceding papers.
4. D.H.E. Gross, Rep Prog. Phys. **53** (1990) 605.
5. M. D'Agostino et al,Phys. Lett. **B371** (1996) 175.
6. W.A. Friedman, Phys. Rev. **C42** (1990) 667.
7. F. Haddad et al, Z. Phys. **A354** (1996) 321.
8. E. Suraud et al, Nucl. Phys. **A495** (1989) 73c.
9. W. Bauer et al, Phys. Rev. Lett. **69** (1992) 1888.
10. B. Borderie et al, Phys. Lett. **B302** (1993) 15.
11. L.G. Moretto et al., Phys. Rev. Lett. **69** (1992) 1884.
12. P. Bonche et al, Nucl. Phys. **A436** (1985) 265.
13. S. Ayik and C. Grégoire Phys. Lett. **B212** (1988) 269; Nucl. Phys. **A513** (1990) 187.
14. J. Randrup and B. Remaud, Nucl. Phys. **A514** (1990) 339.
15. A. Guarnera et al, Proc. XXXIII Intern. Winter Meeting in Nuclear Physics, Bormio, Italy (1995), ed. I. Iori, Riserca scientifica ed educazione permanente, page 293.
16. A. Guarnera, PhD thesis, Caen (1996).
17. B. Jacquot et al, Phys. Rev **C54** (1996) 3025.
18. J. Pouthas et al, Nucl. Inst. and Meth. **A357** (1995) 418.
19. M.F. Rivet for the INDRA collaboration, Proc. of the Int. Workshop on Multiparticle correlations and nuclear reactions, CORINNE II, Nantes, France, 6-10 sept. 1994, ed. J. Aichelin and D. Ardouin, World Scientific 1995, page 338.
20. B. Borderie *et al.*, Phys. Lett. **B205** (1988) 26; M.F. Rivet et al., Proc. XXXI Intern. Winter Meeting in Nuclear Physics, Bormio, Italy (1993), ed. I. Iori, Riserca scientifica ed educazione permanente, page 92.
21. J. Péter et al, Nucl. Phys. **A593** (1995) 95.
22. J.C. Steckmeyer *et al.*, Preprint LPCC 95–13.
23. R. Bougault *et al.*, Nucl. Phys. **A587** (1995) 499.
24. V. Métivier *et al.*, Proc. of the ACS Nucl. Chem. Symp., Anaheim, CA, April 1995.
25. J.L. Charvet and the INDRA collaboration, this meeting.
26. J. Péter et al, Phys. Lett. **B237** (1990) 187.
27. L. Stuttgé *et al.*, Nucl. Phys. **A539** (1992) 511.
28. C.P. Montoya *et al.*, Phys. Rev. Lett. **73** (1994) 3070.
29. J.F. Lecolley et al, Phys. Lett. **B354** (1995) 202.
30. J. Tõke *et al.*, Phys. Rev. Lett. **75** (1995) 2920; **A583** (1995) 519c.
31. W. Lynch, Nucl. Phys. **A583** (1995) 471c.
32. J.E. Sauvestre *et al.*, Phys. Lett. **B335** (1994) 300.

33. J. Łukasik and the INDRA collaboration, Phys. Rev. C in press.
34. J. Frankland and the INDRA collaboration, this meeting.
35. J.F. Lecolley et al, Phys. Lett. **B387** (1996) 460.
36. C.O. Bacri et al., Proc. XXXIV Intern. Winter Meeting in Nuclear Physics, Bormio, Italy (1996), ed. I. Iori, Riserca scientifica ed educazione permanente, page 46.
37. B. Jouault et al, Nucl. Phys. **A591** (1995) 497.
38. R. Bougault, A. Chbihi, S. Salou J.P. Wieleczko and the INDRA collaboration, unpublished data.
39. N. Marie, PhD thesis, Caen 1995.
40. N. Marie and the INDRA collaboration, Phys. Lett. **B391** (1997) 15.
41. D. Durand, code SIMON, in preparation.
42. D. Durand and A. D. Nguyen, private communication.
43. E. Wigner, Trans. Faraday Soc. **34** (1938) 29; L.G. Moretto, Nucl. Phys. **A427** (1975) 211.
44. M. D'Agostino et al, Phys. Lett. **B368** (1996) 259.
45. F. Haddad, F. Sébille, B. Borderie, M.F. Rivet, private communication.
46. A. Guarnera, private communication.
47. R. Bougault for the INDRA collaboration, this meeting.
48. J.L. Charvet and the INDRA collaboration, unpublished data.
49. J.P. Wieleczko, W. Friedmann and R. Bougault, unpublished data.
50. D. Durand et al, preprint LPCC 96-02
51. B. Borderie, Proc. Inter, Symposium on Large-Scale Collective Motion of Atomic Nuclei, Brolo (Messina) Italy, October 1996.
52. A. Bonasera, F. Gulminelli and J. Molitoris, Phys. Rep. **243** (1994) 1.
53. A. Guarnera et al,Proc. XXXIV Intern. Winter Meeting in Nuclear Physics, Bormio, Italy (1996), ed. I. Iori, Riserca scientifica ed educazione permanente, page 68.
54. M.F. Rivet, J. Frankland and the INDRA collaboration, unpublished data.
55. L.G. Moretto et al preprint LBNL-39388 (1996), submitted to Phys. Reports.